Three-dimensional transition characteristics in the wake of an inclined flat plate

Three-dimensional transition characteristics in the wake of an inclined flat plate

D Yang[1], B Pettersen[1], H I Andersson[2] and V D Narasimhamurthy[2]

[1] Department of Marine Technology, NTNU, NO-7491 Trondheim, Norway
[2] Department of Energy and Process Engineering, NTNU, NO-7491 Trondheim, Norway

E-mail: dan.yang@ntnu.no

Abstract. The transition phenomena in the wake of an inclined flat plate at angle of attack 25 degrees are investigated numerically. The Reynolds number, based on the free-stream velocity, plate width and kinematic viscosity, between 275 and 800 has been considered. The Strouhal number versus Reynolds number curves were plotted and compared with two-dimensional simulation data. In the present three-dimensional simulation results, for Reynolds number above 350, the Strouhal numbers converge to a constant value and multiple basic frequencies are detected at certain Reynolds numbers. The spanwise wavelength of secondary structure is estimated by using the autocorrelation method. In the range of Reynolds numbers investigated the spanwise wavelengths, non-dimensionalized by the plate projected width, have a constant value which is consistent with the second instability wavelength detected in the case with the plate normal to the flow.

1. Introduction

The bluff body wake flow is a topic of both theoretical and practical importance. The wake transition from two- (2D) to three-dimensions (3D) has been one of the most outstanding subjects of wake flow and have interested researchers for a long time. A number of investigations have been done in this area both experimentally and numerically.

Square and circular cylinders are the most commonly used geometries to study the wake transition. It has been investigated and reported in detail by (Williamson, 1988, 1992, 1996*a*,*b*), (Barkley & Henderson, 1996), (Zhang *et al.*, 1995), (Luo *et al.*, 2003, 2007), and (Tong *et al.*, 2008). Briefly, the square and circular cylinders wake transition behavior both involves two modes of small-scale three-dimensional instabilities, called mode A and mode B. The critical Reynolds numbers for the inception of these instability modes were identified through the determination of discontinuities in the $St - Re$ curves.

For square cylinder wakes, a critical Reynolds number of approximately 160 and 204 was found for transition to mode A and mode B instability, respectively. These critical Reynolds numbers are lower than their circular cylinder counterparts, which are 180 and 260 for mode A and mode B. The observed spanwise wavelengths for the two modes in square cylinder flows ($5.2D$ and $1.2D$ for mode A and mode B, respectively, where D is the side length of the square cylinder) are longer than their counterparts in circular cylinder flows (3-4D and 0.8-1D, respectively, where D is the cylinder diameter).

Tong *et al.* (2008) investigated the transition phenomena in the wake of an inclined square cylinder, in which mode A and B are present at all six different angles of attack investigated, and the spanwise wavelength shows an angle of attack dependence. According to the short review of Thompson *et al.* (2006) the flow past a flat plate normal to the flow undergoes a transition of two unstable modes at Reynolds number around 105-110 and 125, and has a wavelength of approximately 5-6d and 2d for the two modes (where d is the plate width).

In the present work, the transition behavior of flow past the inclined flat plate in Reynolds number range of 275-800 is investigated. The angle of attack is chosen as 25 degrees as in Zhang *et al.* (2009) in which the two-dimensional simulations show that the transition route from laminar to chaotic flow is very complicated at angle of attack around 20-30 degrees. The three-dimensional simulations presented in this paper show very complex instabilities at angle of attack 25 degrees.

2. Numerical implementations

We consider the incompressible flow past a flat plate inclined to the uniform free-stream, as shown in Figure 1.

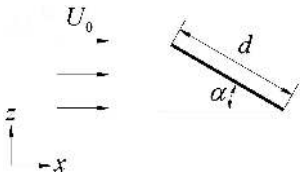

Figure 1: Sketch of free-stream past an inclined flat plate

The control parameter Reynolds number is defined in this paper as $Re = U_0 d/\nu$, where U_0 is the free-stream velocity, d is the plate width, and ν is the kinematic viscosity. The angle of attack is α. We also define the Strouhal number $St = fd/U_0$ for later use, where f is the dominant frequency of the unsteadiness. The non-dimensional 3D Navier-Stokes equations are solved directly. The flow field is described in a coordinate system where x is aligned with the free stream direction, y is along the span of the plate and z is normal to the free-stream (see Figure 1).

The equations are discretized in space by means of the finite-volume method with the grid arranged staggered. The spatial discretization of the convective and diffusive fluxes is based on second-order central differences. The momentum equations are advanced in time by fractional time stepping using a third-order Runge-Kutta scheme. For the accommodation of the flat plate in the Cartesian grid an immersed boundary technique is used. The plate geometry is represented by a triangular mesh. The immersed boundary technique provides a smooth representation of the body surface by using third-order least squares interpolation for the interface cells (Peller *et al.*, 2006).

The computational domain is $25d \times 6d \times 15d$ in x, y and z direction. The inflow plane is located $5d$ upstream from the mid-point of the front face of the plate. The number of grid points is $576 \times 72 \times 450$ with the smallest grid size $0.005d$ around the plate surface. The computed time step is $0.001d/U_0$.

At the inlet, a uniform free-stream velocity profile ($u = U_0$, $v = w = 0$) is assumed. At the outlet boundary, the Neumann boundary condition ($\partial u_i/\partial x = 0$) is used for all the velocity components. No-slip conditions are prescribed at the plate surface. At the top and bottom boundaries, we adopt the slip wall condition ($\partial u/\partial z = \partial v/\partial z = \partial p/\partial z = 0$, $w = 0$). In the spanwise direction, a periodic boundary condition is imposed.

3. Results and discussion

3.1. $St - Re$ relation and velocity-time traces in the wake

The $St - Re$ relation in the Reynolds number range investigated is shown in Figure 2. For comparison the 2D numerical data of Zhang *et al.* (2009) are also plotted. The discrepancy in the St data arises as the Reynolds number is increased above approximately 400 where the 2D simulations give higher frequencies. In the present simulations the 3D effect appears between $Re = 275$ and $Re = 300$, at the same time the subharmonic frequency $f_1/2$ is excited. This subharmonic frequency is also excited in the 2D simulations but at $Re = 320$.

With increase of Re in the 2D simulations, two- and three-frequency (f_2 and f_3) quasi-periodic flow states are generated, for instance at $Re = 600$ and $Re = 700$. The emergence of these multiple basic frequencies is at $Re = 400$ in the 3D simulations. Instead a wideband spectrum near the $f_1/2$ frequency appears at higher Reynolds numbers. Figure 3(a) shows the spanwise averaged power spectrum of the crosswise velocity component at $Re = 400$, in which the second basic frequency f_2 is excited. Spectral peaks in Figure 3(a) occur in linear combinations of the two frequencies related by $m_1(f_1/2) \pm m_2 f_2$, with m_1 and m_2 as integers (Zhang *et al.*, 2009). Figure 3(b) compares the wideband spectrum of spanwise velocity at higher Re with the spectrum at $Re = 350$.

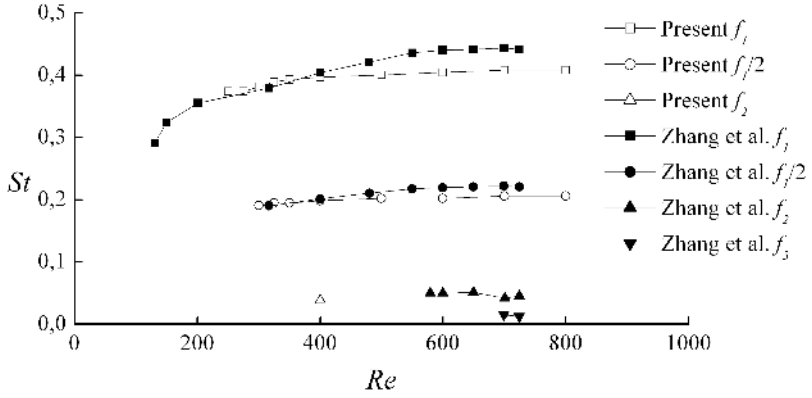

Figure 2: The $St - Re$ relationship in the wake transition regime. The present simulations are 3D, the simulations in Zhang *et al.* (2009) are 2D.

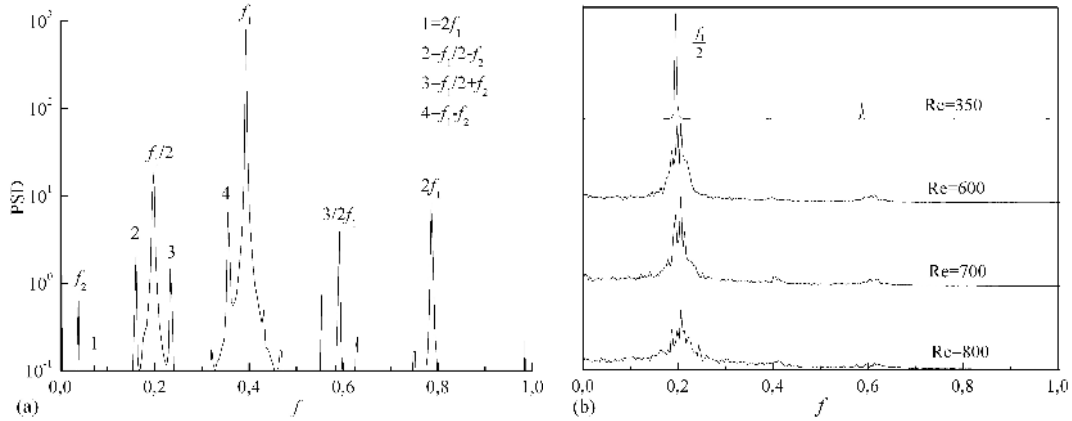

Figure 3: Spanwise averaged spectra of (a) the crosswise velocity component at $Re = 400$, (b) the spanwise velocity component at different Re.

3.2. Instantaneous vortex structure

In this section, three-dimensional vortex structures formed in the wake of the inclined flat plate are also investigated in detail. At $Re = 350$, the regular streamwise-oriented vortical structures,

also referred to as ribs, are generated. Figure 4 shows the top view of an instantaneous 3D iso-surface of $-\lambda_2$ at $Re = 350$, which indicates the spanwise periodicity. The superiority of this method is discussed in detail in Jeong & Hussain (1995). The streamwise vortex structures appear at the same spanwise location during alternate shedding cycles. This scenario implied a spanwise subharmonic behavior, which corresponds to the excitation of the $f_1/2$ frequency.

It should be noted that this spanwise periodicity at lower Re is not equally distributed along the spanwise direction as it is at $Re = 350$. From the top view at $Re = 325$ in Figure 5, it is obvious that the periodic structures along the spanwise direction have a different length scale. Figure 5 indicates two length scales approximately equal to $0.5d$ and $0.8d$, which represent the small and large structures, respectively. The other structure scales are distributed between these two values. These two types of structures appear staggered along the spanwise direction, with a distance between them around $3d$. These non-equidistant spanwise vortex structures suggest that as Re is lower than 350, the 3D instability is not sufficiently strong to form identical streamwise structures along the span. In some positions along the plate span, the 3D scales are relatively small and the generated in-line streamwise vortices are very weak, which leads to a discontinuous distribution of the streamwise structures in the wake.

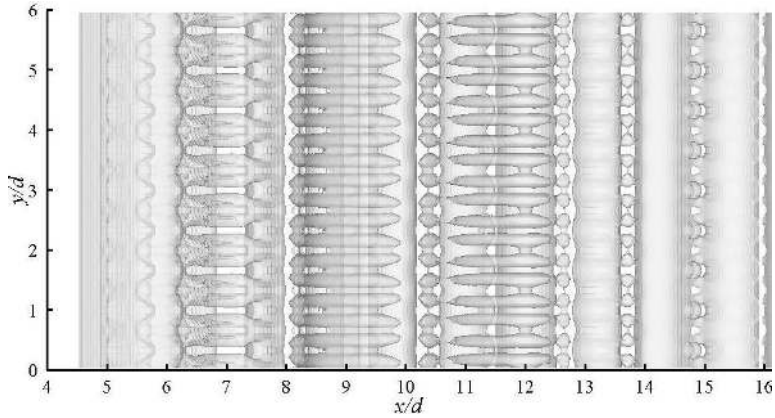

Figure 4: Instantaneous iso-surface of $-\lambda_2$ at $Re = 350$. (The midpoint of the plate is at $x/d = 5$.)

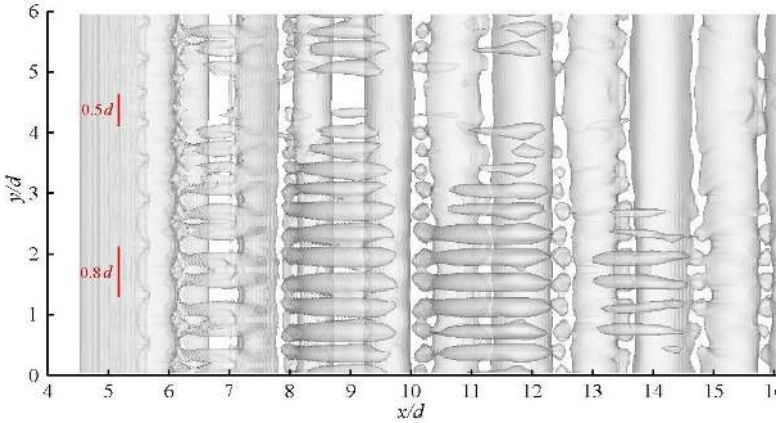

Figure 5: Instantaneous iso-surface of $-\lambda_2$ at $Re = 325$. (The midpoint of the plate is at $x/d = 5$.)

3.3. Spanwise wavelength

The spanwise wavelength (Λ) is estimated by using the two-point correlation function in the spanwise direction. In the current study the autocorrelation function of the spanwise velocity

signal at 72 points in the spanwise direction was used to compute the wavelength. The correlation used here is defined as

$$R_{vv}(l,t) = \frac{\frac{1}{N}\sum_{y=1}^{N} v(y,t)v(y+l,t)}{\frac{1}{N}\sum_{y=1}^{N} v^2(y,t)} \tag{1}$$

where N is the number of points per record and l is the spatial shift.

The calculated autocorrelation function was searched for the first maximum, which measured the instantaneous wavelength $\Lambda(t)$. The wavelengths at different Re are obtained by calculating the highest probability of occurrence of $\Lambda(t)$ (Mansy *et al.*, 1994). Each value is achieved from 300 non-dimensional time units. The data shown in Figure 6(a) are non-dimensionalized by the projected width $d' = d\sin(\alpha)$ for the present inclined flat plate case.

Thompson *et al.* (2006) indicated that two unstable modes were found in the wake flow past a normal flat plate. These two modes have longer and shorter dominant wavelength of $\Lambda = 5-6d$ and $\Lambda \approx 2d$, respectively. In the present investigation, the spanwise wavelength calculated from the time-trace of the three velocity components at the Reynolds number range investigated are all distributed around $\Lambda/d' \approx 2.0$ (Figure 6(a)), which is consistent with the second instability mode A observed by Thompson *et al.* (2006) at $Re \approx 125$.

Figure 6(b) exhibits the probability density function (PDF) of Λ, which is taken from the streamwise velocity component at $Re = 400$. From Figure 2 we know that two basic frequencies coexist at this Re and the other frequency peaks are the linear combination of f_2 and $f_1/2$. The PDF peaks in Figure 6(b) correspond to $\Lambda = 0.87494, 1.77013$ and 2.7491. The spanwise vortex structures corresponding to these three dominant wavelengths will produce different frequency peaks in Figure 3(a). The red line in Figure 6(b) is the fitting curve of the PDF. The fitting function is a summation of four Gaussian functions with different parameters, such as

$$PDF(\Lambda) = \sum_{i=1}^{4} a_i \exp(-(\frac{\Lambda - b_i}{c_i})^2) \tag{2}$$

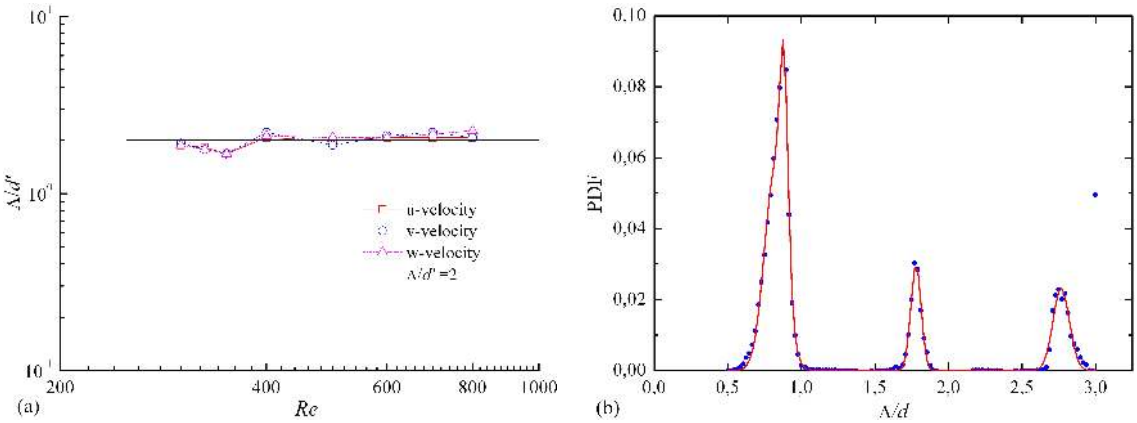

Figure 6: (a)The spanwise wavelength versus Reynolds number at $x/d = 6.0$ and $z/d = 8.0$. (b) PDF distribution of spanwise wavelength taken from the streamwise velocity, $Re = 400$.

4. Conclusions

Three-dimensional numerical simulations have been employed to investigate the transition phenomena in the wake of a flat plate, which is inclined to the free-stream at an angle of attack of 25 degrees. As the Reynolds number increased above 350 the present numerical results give a nearly constant Strouhal number, which is lower than the two-dimensional simulation

results reported earlier. At the early stage of the occurrence of the three-dimensional effects, the streamwise vortices are not equally distributed along the spanwise direction, which is due to the relative small spanwise scale induced on the spanwise vortices.

As Re is increased to 350, identical streamwise vortices are formed along the spanwise direction. With further increase of Re, more than one basic frequency is excited, for example at $Re = 400$, which is accompanied by multiple dominant spanwise wavelengths. By using the autocorrelation method, the spanwise wavelength was estimated, each from the three velocity component time histories over 300 non-dimensional time units. The calculations indicate that the spanwise wavelength non-dimensionalized by the projected width of the plate, approximately maintains a constant value 2.0 at all Reynolds numbers investigated. This value is in good agreement with the second instability wavelength detected in the Floquet analysis of the normal flat plate flow case.

From the detailed analysis, the transition characteristics in the wake of an inclined flat plate could be described as follows: In the early stage of the transition the three-dimensional effects are not strong enough to form equivalent streamwise vortices along the spanwise direction. The Strouhal numbers initially increase with Reynolds number. As the secondary structures are formed equally in the wake, the Strouhal numbers reach a constant value. It has been conclusively shown that the spanwise wavelength remains almost constant in the entire transition process, and the probability density functions have the same form as the Gaussian function.

References

Barkley, D. & Henderson, R. D. 1996 Three dimensional Floquet stability analysis of the wake of circular cylinder. *J. Fluid Mech.* **322**, 215–241.

Jeong, J. & Hussain, F. 1995 On the identification of a vortex. *J. Fluid Mech.* **285**, 69–94.

Luo, S. C., Chew, Y. T. & Ng, Y. T. 2003 Characteristics of square cylinder wake transition flows. *Phys. Fluid* **15**, 2549–2559.

Luo, S. C., Tong, X. H. & Khoo, B. C. 2007 Transition phenomena in the wake of a square cylinder. *J. Fluids Struct.* **23**, 227–248.

Mansy, H., Yang, P.-M. & Williams, D. R. 1994 Quantitative measurements of three-dimensional structures in the wake of a circular cylinder. *J. Fluid Mech.* **270**, 277–296.

Peller, N., Duc, A. L., Tremblay, F. & Manhart, M. 2006 High-order stable interpolations for immersed boundary methods. *Int. J. Numer. Meth. Fluids* **52**, 1175–1193.

Thompson, M. C., Hourigan, K., Ryan, K. & Sheard, G. J. 2006 Wake transition of two-dimensional cylinders and axisymmetric bluff bodies. *J. Fluids Struct.* **22**, 793–806.

Tong, X. H., Luo, S. C. & Khoo, B. C. 2008 Transition phenomena in the wake of an inclined square cylinder. *J. Fluids Struct.* **24**, 994–1005.

Williamson, C. H. K. 1988 The existence of two stages in the transition to three dimensionality of a circular cylinder wake. *Phys. Fluid* **31**, 3165–3168.

Williamson, C. H. K. 1992 The natural and forced formation of spot-like 'vortex dislocations' in the transition of a wake. *J. Fluid Mech.* **243**, 393–441.

Williamson, C. H. K. 1996*a* Three-dimensional wake transition. *J. Fluid Mech.* **328**, 345–407.

Williamson, C. H. K. 1996*b* Vortex dynamics in the cylinder wake. *Annu.Rev. Fluid Mech.* **28**, 477–539.

Zhang, H., Fey, U., Noack, B. R., Konig, M. & Eckelmann, H. 1995 On the transition of the cylinder wake. *Phys. Fluid* **7**, 779–794.

Zhang, J., Liu, N.-S. & Lu, X.-Y. 2009 Route to a chaotic state in fluid flow past an inclined flat plate. *Phys. Rev. E* **79**, 045306.